

chemistry are few in number.<sup>27</sup> In the present study, oxidation of turbostratic BN samples obtained from 2 and 6 (vacuum pyrolysis at 900 °C, pyrolysis at 1200 °C under N<sub>2</sub>) was studied by TGA in air. A typical curve for 6 is shown in Figure 2. The samples show no weight gain or loss from 50 to ~900 °C. Above 900 °C, an abrupt weight gain corresponding to oxidation of the BN occurs. Above ~1050 °C, a weight loss occurs that corresponds to volatilization of the boron oxide species formed in the oxidation process. More detailed examinations of the oxidation behavior of other turbostratic and highly ordered h-BN samples are in progress that address the effects of crystallinity, surface area, and other features on oxidation characteristics.<sup>30</sup>

### Conclusion

This study shows that a series of two-point poly(borazinylamine)s, protected from three-point polymerization by a NMe<sub>2</sub> group on each borazine monomer unit, can be prepared and used as oligomeric precursors to form turbostratic boron nitride powder that contains small (1–5%)

carbon impurity. The ceramic products obtained under several pyrolysis conditions are sensitive to air oxidation above ~900 °C. Further, it is found that the majority of dimethylamino protecting groups may be readily removed from the two-point oligomer 1 at room temperature by treatment of the gel with H<sub>3</sub>B·THF. The resulting oligomer is converted to turbostratic BN in good yield (55–60%) with or without the use of NH<sub>3</sub> in the pyrolysis atmosphere, and carbon impurities are negligible. Although these reagents have been found to be useful only for the preparation of BN powders, the results suggest additional chemical modifications that should provide fusible or soluble polymeric precursors.

**Acknowledgment.** Financial assistance for this study was provided by Sandia National Laboratory (Contract 55-7566) and the National Science Foundation (Grant CHE-8503550). A DOE contract (DE-FG05-86ER75294) provided support for the purchase of the high-field NMR spectrometer used to characterize the soluble borazine compounds.

**Registry No.** BN, 10043-11-5;  $[(CH_3)_3Si]_2NCH_3$  (2-(dimethylamino)-4,6-dichloroborazine (copolymer), 127491-80-9;  $[(CH_3)_3Si]_2(2\text{-dimethylamino})$ -4,6-dichloroborazine (copolymer), 127516-89-6.

(30) Borek, T. T.; Lindquist, D. A.; Johnston, G. P.; Hietala, S. L.; Smith, D. M.; Paine, R. T., to be published.

## Oxygen-17 Nuclear Magnetic Resonance Studies of Lanthanum Strontium Copper Oxide

Marjorie S. Went and Jeffrey A. Reimer\*

Center for Advanced Materials, Lawrence Berkeley Laboratory, and Department of Chemical Engineering, University of California at Berkeley, Berkeley, California 94720-9989

Received January 3, 1990

We have obtained oxygen-17 nuclear magnetic resonance spectra of La<sub>1.85</sub>Sr<sub>0.15</sub>CuO<sub>4</sub> at temperatures ranging from 12 to 295 K. We observe three resonances and assign them to planar oxygen sites, axial oxygen sites, and a satellite peak of the lanthanum-139 resonance. Temperature-dependent studies of the resonance frequency associated with the axial site show that this resonance moves to higher frequency just above the critical temperature and then rapidly shifts to lower frequency upon formation of the superconducting state. It is suggested that the spin susceptibility of this oxygen site is affected by the onset of superconductivity. Spin-lattice relaxation of this resonance appears to be dominated by quadrupolar mechanisms at temperatures above the critical temperature; the relaxation rate is nearly constant below the critical temperature.

### Introduction

The discovery of superconductivity above 30 K in alkaline-earth-metal-substituted lanthanum copper oxides in 1986<sup>1</sup> has led to numerous research efforts aimed at characterizing and understanding the mechanism of high-temperature superconductivity in these materials. Because oxygen plays a key role in the superconducting mechanism as well as in the processing of these oxides, we decided to probe the microstructure around the oxygen nuclei using oxygen-17 nuclear magnetic resonance (NMR) experiments. Of the many high-temperature superconducting oxides discovered in the last few years, the lanthanum copper oxide systems lend themselves particularly well to oxygen-17 NMR studies because of their relatively

simple crystal structures and high symmetry around the two distinct oxygen sites. Furthermore, we hoped that an increased understanding of the role of oxygen in these systems would assist the efforts at understanding superconductivity in more complex systems that superconduct at higher temperatures.

NMR measurements of the spin-lattice relaxation rates ( $1/T_1$ ) and the Knight shift ( $K$ ) can provide local, microscopic information on the spin dynamics in these materials. In particular, we surmised that determination of the spin-lattice relaxation rates above and below the critical temperature would give a localized measure of the density of states at the Fermi level and of the superconducting bandgap.<sup>2</sup> In metallic compounds where relaxation pro-

\* To whom correspondence should be addressed at the Department of Chemical Engineering.

(1) Bednorz, J. G.; Müller, K. A. *Z. Phys. B* 1986, 64, 189.  
(2) Hebel, L. C.; Slichter, C. P. *Phys. Rev.* 1957, 113, 1504.

ceeds via the conduction electrons, the relaxation rate as a function of temperature obeys the Korringa relationship:<sup>3</sup>

$$T_1 T = (\hbar / (4\pi k)) (\gamma_e / \gamma_n)^2 (H / \Delta H)^2 = \text{constant} \quad (1)$$

where  $\gamma_e$  and  $\gamma_n$  are the electron and nuclear gyromagnetic ratios and  $H / \Delta H$  is the ratio of applied field to field enhancement, proportional to the density of states at the Fermi level, as discussed below. This type of behavior has been seen above the critical temperature in the yttrium-89 relaxation rates<sup>4</sup> but not in the copper relaxation rates in  $\text{YBa}_2\text{Cu}_3\text{O}_{7-x}$ .<sup>5-9</sup> In a conventional BCS superconductor, the relaxation rate is an exponential function of inverse temperature below the critical temperature, with the Arrhenius slope providing a measure of the superconducting bandgap.<sup>2</sup>

The Knight shift is an enhancement of the magnetic field felt at the nucleus resulting from the alignment of conduction electron spins with the applied field. It is a sum of contributions from spin and orbital magnetic moments. In the superconducting state the Knight shift can be a function of temperature. Because the Van Vleck orbital susceptibility is independent of the spin state of the conduction electrons, it should not be changed by pairing in the superconducting state. The remaining spin term can be expressed as

$$K_s = \Delta\omega / \omega_0 = (8\pi/3) [U_F(0)]^2 \chi \quad (2)$$

where  $\Delta\omega$  is the frequency shift relative to  $\omega_0$ , the frequency of a diamagnetic reference,  $[U_F(0)]^2$  is the probability amplitude of the electron wave function at the nucleus, and  $\chi$  is the Pauli spin susceptibility, proportional to the density of states at the Fermi level.<sup>10</sup> The Knight shift expressed in ppm is usually positive (higher frequency than a diamagnetic reference) and independent of the applied field strength. The non-s character of electron wave functions can also produce a field at the nucleus due to the "core-polarization effect".<sup>11</sup> The Knight shift is then expressed as<sup>12</sup>

$$K_s = \alpha \chi_s + \gamma \chi_{\text{non-s}} \quad (3)$$

where  $\chi_s$  and  $\chi_{\text{non-s}}$  refer to the s and non-s spin contributions to the susceptibility. When nuclei are associated with atoms in which covalent bonding is involved, s and non-s should properly refer to the angular momenta of the molecular orbitals. In the superconducting state,  $\chi_s$  and  $\chi_{\text{non-s}}$  are temperature dependent at temperatures where  $kT$  is close to the value of the superconducting bandgap. The coefficient  $\gamma$  is often negative.<sup>12</sup> In materials where  $\chi_{\text{non-s}}$  is negligible, Yosida<sup>13</sup> accounted for Knight shift

behavior below  $T_c$  using BCS theory. In Yosida's analysis all ground-state pairs are either occupied or not and hence contribute nothing to the spin susceptibility. Only pair-excited states contribute to the susceptibility, resulting in an exponential dependence of  $K_s$  upon temperature below  $T_c$ .

Much evidence has been accumulating that the charge carriers that contribute to the density of states at the Fermi level in high- $T_c$  copper oxides are holes with dominant O(2p) character.<sup>14-16</sup> Observations of Knight shifts and relaxation rates in  $\text{YBa}_2\text{Cu}_3\text{O}_{7-x}$  have provided valuable information on the spin states and spin dynamics in this material.<sup>4,5,17-21</sup> Recent analysis of the positive copper-63 Knight shift observed in  $\text{YBa}_2\text{Cu}_3\text{O}_{7-x}$  has shown that the spin susceptibility of both the plane and chain copper sites is affected by the onset of superconductivity.<sup>19</sup> It was suggested by these authors that significant contributions arise from the oxygen p states. Exponential Yosida behavior<sup>13</sup> was observed at the Cu(I) sites (chains), indicative of isotropic pairing.<sup>19</sup> A negative Knight shift was observed for yttrium-89 in  $\text{YBa}_2\text{Cu}_3\text{O}_{7-x}$ , which decreases (shifts to lower frequency) on going to the superconducting state.<sup>4,17</sup> On the basis of this observation, these authors hypothesize that a  $\sigma$  hybridization of the Cu(3d) and O(2p) holes contributes to the electron wave function at the Fermi level.<sup>18,20</sup> Other oxygen-17 NMR studies of the isotropic and anisotropic shift in  $\text{YBa}_2\text{Cu}_3\text{O}_{7-x}$  have led to the conclusion that the holes reside in  $\sigma$  orbitals (deriving from the p atomic orbitals of oxygen), with lobes along the Cu-O bond axis in the planar and bridging oxygen sites, and that these O(p) states along with the Cu(d) states contribute to the spin density.<sup>22</sup> A shift to lower frequency below  $T_c$  was also observed in the oxygen-17 spectrum of the  $\text{CuO}_2$  plane sites in  $\text{YBa}_2\text{Cu}_3\text{O}_{7-x}$ .<sup>23</sup>

In this paper we report our observations and interpretations of the oxygen-17 NMR parameters from the lanthanum copper oxide system. We find that resonances associated with both oxygen sites are distinguishable from a broad background signal emanating from satellite transitions of the lanthanum-139 nucleus. The oxygen resonance associated with  $\text{CuO}_2$  plane oxygen sites is quite broad and difficult to quantitatively characterize. The NMR spectra of the axial oxygens in the La(Sr)O planes, however, are narrow and tractable to spectroscopic analysis. Hence we proceeded to investigate their temperature-dependent NMR parameters. Our oxygen-17 experiments indicate that spin-lattice relaxation is not Korringa-like at any temperature but is dominated by quadrupolar effects.  $T_1$  measurements below  $T_c$  are obfuscated by the overlapping resonance of the lanthanum-139 nuclei, which exhibit shorter relaxation times. We observed a diamagnetic (low frequency) shift in the resonance position of the axial oxygens as the samples were cooled below the critical temperature. We conclude that this observed

(3) Korringa, J. *Physica (Amsterdam)* 1950, 16, 601.  
 (4) Markert, J. T.; Noh, T. W.; Russek, S. E.; Cotts, R. M. *Solid State Commun.* 1987, 63, 847.  
 (5) Pennington, C. H.; Durand, D. J.; Slichter, C. P.; Rice, J. P.; Borkowski, E. D.; Ginsberg, D. M. *Phys. Rev. B* 1989, 39, 2902.  
 (6) Walstedt, R. E.; Warren, W. W., Jr.; Bell, R. F.; Brennert, G. F.; Espinosa, G. P.; Remeika, J. P.; Cava, R. J.; Rietman, E. A. *Phys. Rev. B* 1987, 36, 5727.  
 (7) Furo, I.; Jánossy, A.; Mihály, L.; Banki, P.; Pócsik, I.; Bakonyi, I.; Heinmaa, I.; Joon, E.; Lippmaa, E. *Phys. Rev. B* 1987, 36, 5690.  
 (8) Pennington, C. H.; Durand, D. J.; Zax, D. B.; Slichter, C. P.; Rice, J. P.; Ginsberg, D. M. *Phys. Rev. B* 1988, 37, 7944.  
 (9) Warren, W. W., Jr.; Walstedt, R. E.; Brennert, G. F.; Cava, R. J.; Tycko, R.; Bell, R. F.; Dabbagh, G. *Phys. Rev. Lett.* 1989, 62, 1193.  
 (10) Slichter, C. P. *Principles of Magnetic Resonance*; Springer-Verlag: Berlin, 1980.  
 (11) Watson, R. E.; Freeman, A. J. *Hyperfine Interactions*; Freeman, A. J., Frankel, R. B., Eds.; Academic Press: New York, 1967.  
 (12) Winter, J. *Magnetic Resonance in Metals*; Clarendon Press: Oxford, 1971.  
 (13) Yosida, K. *Phys. Rev.* 1958, 110, 769.

(14) Nücker, N.; Fink, J.; Fuggle, J. C.; Durham, P. J.; Temmerman, W. M. *Phys. Rev. B* 1988, 37, 5158.  
 (15) Johnston, D. C.; Sinha, S. K.; Jacobson, A. J.; Newsam, J. M. *Physica C (Amsterdam)* 1988, 153-155, 572.  
 (16) Johnston, D. C. *Phys. Rev. Lett.* 1989, 62, 957.  
 (17) Alloul, H.; Mendels, P.; Collin, G.; Monod, P. *Phys. Rev. Lett.* 1988, 61, 746.  
 (18) Alloul, H.; Ohno, T.; Mendels, P. *Phys. Rev. Lett.* 1989, 63, 1700.  
 (19) Takigawa, M.; Hammel, P. C.; Heffner, R. H.; Fisk, Z. *Phys. Rev. B* 1989, 39, 7371.  
 (20) Adrian, F. J. *Phys. Rev. Lett.* 1988, 61, 2148.  
 (21) Hammel, P. C.; Takigawa, M.; Heffner, R. H.; Fisk, Z.; Ott, K. C. *Phys. Rev. Lett.* 1989, 63, 1992.  
 (22) Takigawa, M.; Hammel, P. C.; Heffner, R. H.; Fisk, Z.; Ott, K. C.; Thompson, J. D. *Phys. Rev. Lett.* 1989, 63, 1865.  
 (23) Oldfield, E.; Coretsopoulos, C.; Yang, S.; Reven, L.; Lee, H. C.; Shore, J.; Han, O. H.; Ramli, E.; Hinks, D. *Phys. Rev. B* 1989, 40, 6832.

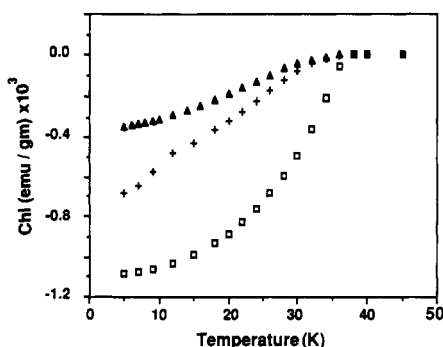


**Figure 1.** Magnetic susceptibility of  $\text{La}_{1.88}\text{Sr}_{0.15}\text{CuO}_4$  as a function of temperature:  $^{17}\text{O}$ -enriched sample I (open squares),  $^{17}\text{O}$ -enriched sample II (solid triangles), and  $^{18}\text{O}$  precursor to sample II (crosses).

temperature-dependent shift is largely contributed to by the Knight shift and speculate, in the context of the above discussion, that it reflects the electronic character of those carriers that are paired to form the superconducting state.

### Experimental Section

The  $\text{La}_{1.88}\text{Sr}_{0.15}\text{CuO}_4$  was prepared by coprecipitation of the metal oxalates. Stoichiometric amounts of  $\text{La}_2\text{O}_3$  (Alfa, 99.99%),  $\text{SrCO}_3$  (Aesar, puratronic), and  $\text{CuO}$  (Fisher, ACS certified) were dissolved in concentrated nitric acid followed by addition of oxalic acid. The mixture was evaporated to dryness. The powder was then fired in a platinum crucible at  $800\text{ }^\circ\text{C}$  in air for 12 h and ground. To prepare the enriched samples, the final annealing was done in a static atmosphere of enriched oxygen (35% oxygen-17, Cambridge Isotope Laboratories) for 12 h at  $950\text{ }^\circ\text{C}$  followed by 4 h at  $500\text{ }^\circ\text{C}$ . For the NMR experiments, it was necessary to disperse the samples as small particles to avoid radio frequency (rf) penetration (skin depth) limitations. The annealed samples were mixed with  $\text{SiO}_2$  (Cab-O-Sil, grade M-5) as the dispersing agent and put in an agate ball mill with hexane added as a solvent. The agate ball mill was shaken for 45 min, and the hexane was then evaporated. This resulted in particles less than  $20\text{ }\mu\text{m}$  in diameter, as determined by examination under a microscope. Two samples were prepared from different starting materials following the above procedure. One of the samples (sample I) was simply placed in an NMR tube. The other (sample II) was heated to  $100\text{ }^\circ\text{C}$  to drive off any water present and then flame sealed in an NMR tube. The percent of oxygen-17 in the samples, determined by temperature-programmed reduction (TPR) measurements of the ratio of evolved  $\text{H}_2^{16}\text{O}$  to  $\text{H}_2^{17}\text{O}$ , was found to be between 20 and 25%. Powder X-ray diffraction (Rigaku Geigenflex, Model 4036V2 diffractometer with  $\text{Cu K}\alpha$  radiation) showed that the enriched and treated sample II has a pattern nearly identical with that of the unenriched sample and is ostensibly pure  $\text{La}_{2-x}\text{Sr}_x\text{CuO}_4$ . Magnetic measurements were performed on a superconducting quantum interference device (SQUID) magnetometer (SHE) in an applied field of 20 G, which was determined by using a calibrated superconducting tin sphere.

The high-field, static NMR experiments were performed on a commercial spectrometer (Nalorac Cryogenics Corp. QUEST 4300) using a wide-bore, 9.4-T magnet (Oxford Instruments). Frequencies are referenced to the resonance of oxygen-17 (spin  $5/2$ , natural abundance = 0.04%) in enriched  $\text{H}_2\text{O}$  at 54.12 MHz by using the IUPAC  $\delta$  scale (positive numbers represent higher frequencies).<sup>24</sup> The data were taken by using the Hahn echo sequence (90°-τ-180°-τ-echo), to observe the central transition of the quadrupolar line shape.<sup>25</sup> Solid 90° pulse lengths were

(24) The  $^1\text{H}$  resonance arising from the hydroxyl groups on the  $\text{SiO}_2$  in sample II was measured between 12 and  $295\text{ K}$  to correlate any temperature-dependent field shifts not arising from the internal interactions at the  $^{17}\text{O}$  nuclei. A linear shift (adjusted to 0 ppm at  $295\text{ K}$ ) was found:  $\sigma$  (ppm) =  $0.26 T(\text{K}) - 75.83$  ( $R^2 = 0.98$ ). The reported  $^{17}\text{O}$  data reflect subtraction of this shift. We also note that a slight broadening of the hydroxyl  $^1\text{H}$  resonance was observed as the temperature was decreased.

(25) Abragam, A. *Principles of Nuclear Magnetism*; Clarendon Press: Oxford, 1961.

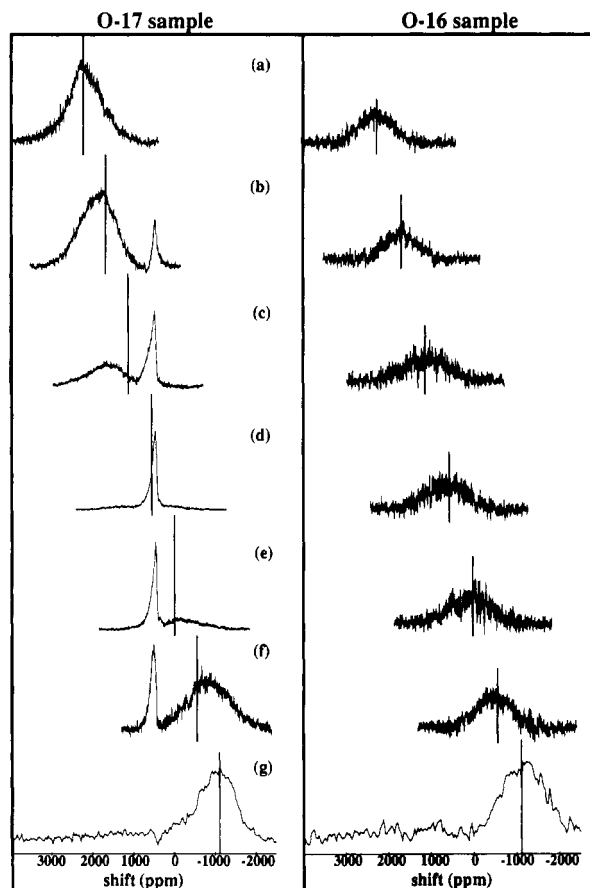


**Figure 2.** NMR spin-echo spectra of  $^{17}\text{O}$ -enriched  $\text{La}_{1.88}\text{Sr}_{0.15}\text{CuO}_4$  (sample II) and of unenriched ( $^{18}\text{O}$ )  $\text{La}_{1.88}\text{Sr}_{0.15}\text{CuO}_4$ . The spectrometer frequency was centered at (a) 120, (b) 90, (c) 60, (d) 30, (e) 0, (f) -30, (g) -60 kHz relative to the resonance of  $\text{H}_2\text{O}$ . Vertical lines are drawn at the spectrometer frequency. The sweep width was  $\pm 100$  kHz in a-f and  $\pm 1$  MHz in g. Intensities are scaled arbitrarily.

approximately  $6\text{ }\mu\text{s}$  and delay times were  $150\text{ }\mu\text{s}$ . The sweep width of the spectrometer was 100 kHz. Spectra were taken in the temperature range  $12$ – $295\text{ K}$ . The  $T_1$  measurements were performed using the method of progressive saturation with spin echoes.<sup>26</sup> The magnetization as a function of the delay time between successive acquisitions was fit to an exponential from which the time constant ( $T_1$ ) was extracted. The delay times encompassed a range from approximately  $0.1T_1$  to  $5T_1$ . The magic-angle-spinning NMR spectra were taken on the same instrument with a commercial probe (Doty Scientific Inc.) using simple excitations with one solid  $90^\circ$  pulse. The maximum spinning speed achieved was 4.2 kHz. Additionally, a low-field (6.3 T), static NMR spectrum was taken on a home-built spectrometer at a resonance of 36.2 MHz, at room temperature. The Hahn echo sequence was used with a solid  $90^\circ$  pulse length of  $6\text{ }\mu\text{s}$ .

### Results

Figure 1 shows the magnetic susceptibility as a function of temperature of the enriched and dispersed samples I and II, taken after completion of the NMR experiments, and of the oxygen-16 precursor to sample II. The onset of superconductivity occurs at  $36\text{ K}$  in all three cases. The broadness of the transition in sample II and its slightly lower transition temperature indicate that this sample is of poorer quality. It is likely that in this sample the strontium stoichiometry is not optimum for superconductivity, though the structure, as verified by the X-ray

(26) Fukushima, E.; Roeder, S. B. W. *Experimental Pulse NMR. A Nuts and Bolts Approach*; Addison-Wesley: Reading, MA, 1981.

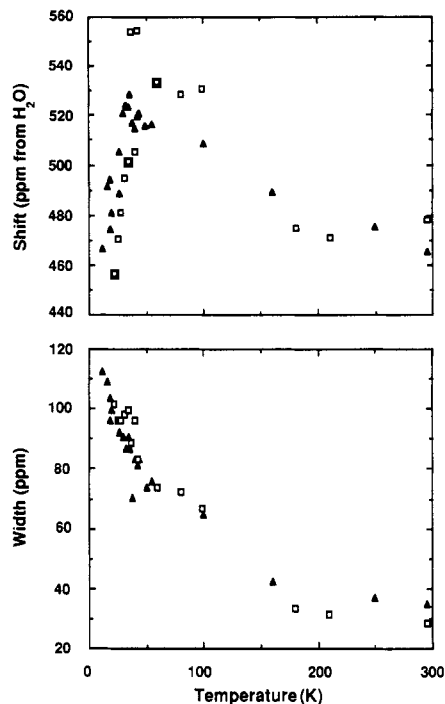
diffraction, remained pure  $\text{La}_{2-x}\text{Sr}_x\text{CuO}_4$ .<sup>27</sup>

Figure 2 shows static spin-echo 54.1-MHz NMR spectra of the oxygen-17-enriched sample II and unenriched  $\text{La}_{1.85}\text{Sr}_{0.15}\text{CuO}_4$  taken at room temperature. In each spectrum, the spectrometer carrier frequency was incremented by 30 kHz. Three features are immediately apparent. In spectra obtained from both enriched and unenriched samples there is a weak resonance that follows the carrier frequency, indicating that it is broader than the band width determined by the length of the  $180^\circ$  pulse (11.5  $\mu\text{s}$ ). This signal is most intense near -1000 ppm. It was confirmed, after performing additional background experiments and integrating peak areas, that this peak is not due to natural-abundance oxygen-17 in background sources such as the  $\text{SiO}_2$ , the sample tube, or the probe. Therefore, this broad signal is attributed to a satellite peak of the resonance of the lanthanum-139 nuclei (spin  $7/2$ ,  $\omega_0 = 56.39$  MHz at 9.4 T, natural abundance = 99.9%). A lanthanum-139 quadrupole coupling constant of 6.1 MHz has been observed in this material, which is large enough to account for a satellite at the oxygen frequency.<sup>28</sup> In support of this assignment, additional intense echoes occurring at  $2\tau$  and  $3\tau$  were observed in the spin-echo raw data at low temperatures. These quadrupolar echoes most likely arise from the lanthanum-139 nuclei, because for the spin  $5/2$  oxygen-17 nuclei the echo at  $3\tau$  is forbidden and thus would have appeared in much lower relative intensity if at all.<sup>25</sup> Next we note the presence of an additional broad peak that appears most intense at about 1800 ppm. This is best seen in Figure 2b, a spectrum taken with the spectrometer carrier frequency centered at 1660 ppm. This peak is absent in the spectra of the unenriched sample, and hence we assign it to oxygen-17. Finally, a well-resolved narrow peak centered at about 475 ppm is observed in samples that are enriched with oxygen-17.

Spin counts were done by comparing the integrated area of a spectrum containing a weighed amount of the enriched  $\text{La}_{1.85}\text{Sr}_{0.15}\text{CuO}_4$  (sample II), taken with a single  $90^\circ$  excitation pulse, with the area of a spectrum of enriched  $\text{H}_2\text{O}$  containing a known number of oxygen-17 nuclei. The integrated area was corrected for the reduced sensitivity of quadrupolar nuclei in solids,<sup>26</sup> finite rf penetration depth,<sup>25</sup> losses of signal due to probe ringdown, and percent isotope exchange as determined by TPR. It was determined that in the narrower peak at 475 ppm, 20–40% of the total spins expected were accounted for. We estimate that the total area of the broad oxygen-17 peak is between 1 and 2 times that of the narrow peak; therefore, roughly all expected spins are accounted for.

We obtained two additional spectra of the region near 500 ppm in sample II. The first was a room-temperature magic-angle-spinning spectrum. This spectrum showed two spinning sidebands symmetrically displaced from one main peak by 4.2 kHz, the spinning speed. The main peak attributed to the oxygen-17 resonance had a Gaussian half-width at half-maximum of 1.2 kHz (22 ppm) that was reduced from 1.6 kHz (30 ppm) in the case of no spinning. The second spectrum was obtained at a lower magnetic field ( $\omega_0 = 36.2$  MHz). The spectral features of the narrow resonance at this lower frequency were identical with those observed at higher frequency; the center of mass was at 537 ppm.

Figure 3 is a plot of the first and second moments of the resonance near 475 ppm as a function of sample temper-



**Figure 3.** Top: centers of mass as a function of temperature for  $^{17}\text{O}$ -enriched  $\text{La}_{1.85}\text{Sr}_{0.15}\text{CuO}_4$ ; sample I (open squares) and sample II (solid triangles). Bottom: line widths as a function of temperature for  $^{17}\text{O}$ -enriched  $\text{La}_{1.85}\text{Sr}_{0.15}\text{CuO}_4$ ; sample I (open squares) and sample II (solid triangles). Line widths represent half-widths at half-maximum intensity. Centers of mass and line widths of the narrow line shape attributed to the axial (O1) oxygen site were determined after subtracting a broad underlying Gaussian due to the lanthanum resonance.

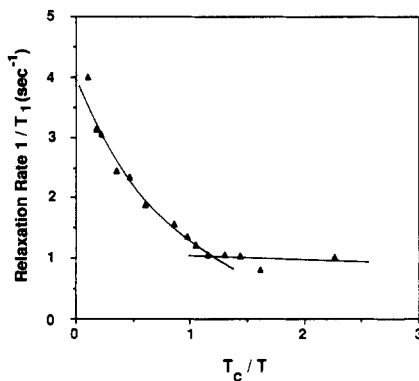


**Figure 4.** Spin-lattice relaxation rate ( $1/T_1$ ) as a function of inverse temperature for the narrow line shape attributed to the axial (O1) oxygen site in  $\text{La}_{1.85}\text{Sr}_{0.15}\text{CuO}_4$  (sample II). The solid line represents an exponential fit to the data above  $T_c$  and a linear fit below  $T_c$ , as described in the text.

ature, for samples I and II. As the temperature decreases, this line clearly broadens and shifts in frequency.

Figure 4 shows the oxygen-17 relaxation rates ( $1/T_1$ ) of the narrow resonance in sample II as a function of inverse temperature ( $T_c/T$ ). For these experiments, the broad peak centered about the spectrometer carrier frequency was fit to a Gaussian and subtracted. The integrated area of the remainder of the spectrum was used to represent the total magnetization for the  $T_1$  calculations.

## Discussion

The static and magic-angle-spinning spectra taken at room temperature with the spectrometer carrier frequency centered at 550 ppm indicate the presence of one well-resolved inhomogeneous line shape arising from the oxygen-17 resonance located at 475 ppm from the resonance

(27) We continue to refer to our sample as  $\text{La}_{1.85}\text{Sr}_{0.15}\text{CuO}_4$  throughout the paper, however.

(28) Lütgemeier, H.; Pieper, M. W. *Solid State Commun.* 1987, 64, 267.

of H<sub>2</sub>O and an additional oxygen-17 resonance centered near 1800 ppm. A broad underlying peak contributed to by the lanthanum-139 resonance appears centered at the carrier frequency. The assignment of the two oxygen resonances follows.

La<sub>1.85</sub>Sr<sub>0.15</sub>CuO<sub>4</sub> possesses the crystal structure of a layered perovskite.<sup>29</sup> Two oxygen sites are present. O1 refers to the axial oxygens in the La(Sr)O planes and O2 to the oxygens in the CuO<sub>2</sub> planes. Others have reported the presence of two oxygen-17 peaks, one located at approximately 500 ppm and one located at approximately 1800 ppm, in La<sub>1.85</sub>Sr<sub>0.15</sub>CuO<sub>4</sub>,<sup>23</sup> YBa<sub>2</sub>Cu<sub>3</sub>O<sub>7-x</sub>,<sup>22,23,30</sup> and other superconducting oxides<sup>23</sup> possessing similar layered perovskite structures. The higher frequency (1800 ppm) resonance has been assigned to the oxygens in the CuO<sub>2</sub> planes, on the basis of rotation patterns, its absence in Cu-free oxides, and its relaxation behavior.<sup>23</sup> Our observations are consistent with these previous studies in that we see two main contributions to the oxygen line shape, in an area ratio of approximately 1:1, at the same positions. Following these works we thus assign the peak at 475 ppm to axial oxygens (O1) and the broader peak at 1800 ppm to oxygens in the CuO<sub>2</sub> planes (O2). We calculated electric field gradients, assuming a point charge model for the lattice,<sup>31</sup> which showed that the quadrupole coupling constants,  $\nu_Q$ , for O1 and O2 are in the ratio of 1:3 and the asymmetry parameter,  $\eta$ , is 0.3 for O2 and 0 for O1. Therefore, if quadrupolar mechanisms dominate, we would expect the broader peak to be due to the O2 oxygens.

Given the difficulty in characterizing NMR parameters for the O2 oxygen site (1800 ppm resonance), we turn our attention to the details of the spectra associated with the axial oxygen site. We find that at room temperature the resonance position is governed by chemical or Knight shifts with some contribution from second-order quadrupolar shifts. At lower temperatures the chemical and Knight shift effects change as the sample goes through its superconducting transition. The characteristic line shape at all temperatures is dominated by chemical and Knight shift anisotropy, with varying contributions from other inhomogeneous mechanisms. The supporting evidence for these conclusions follows.

The internal interactions that may contribute to the line shape, or second moment, associated with the narrow resonance are dipolar effects, second-order quadrupolar broadening, chemical shift anisotropy, and Knight shift anisotropy. The dipolar couplings between the axial oxygen nuclei and copper nuclei or lanthanum/strontium nuclei, separated by bond lengths of 2.41 (Cu-O1) and 1.79 Å (La/Sr-O1),<sup>29</sup> were calculated from the VanVleck formula<sup>32</sup> to produce symmetric, Gaussian broadenings (expressed as half-width at half-maximum intensity) of 7 and 20 ppm, respectively. The actual half-width of the O1 resonance at 295 K is 30 ppm, and the line shape is asymmetric; hence the dipolar interaction is important but not the predominant contributor to the line shape. Second-order quadrupolar effects cause a frequency shift that is positive for oxygen-17 and a broadening, both proportional to  $\nu_Q^2/H_0$ , where  $\nu_Q$  is the quadrupolar coupling constant<sup>33</sup> and  $H_0$  is the applied field strength. The domination of the central transition of the line shape of a

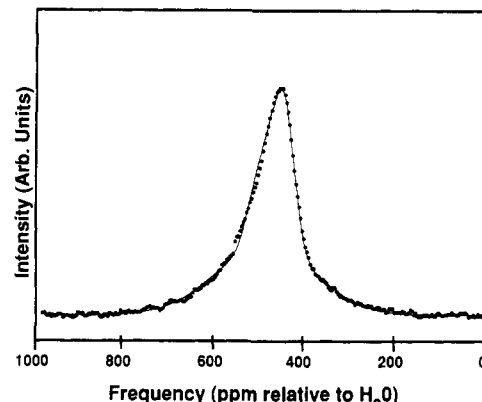


**Figure 5.** Spin-echo spectrum of the resonance attributed to the axial (O1) oxygen site in sample II of La<sub>1.85</sub>Sr<sub>0.15</sub>CuO<sub>4</sub> (dots) and best fit to a chemical or Knight shift powder pattern (solid line). Parameters derived from the fit are described in the text.

quadrupolar nucleus by second-order quadrupolar interactions results in a characteristic powder pattern.<sup>33</sup> This powder pattern was not observed. The static spectra taken at 295 K were fit to (i) a combination of two Gaussians and (ii) a combination of a Gaussian and an asymmetric chemical (or Knight) shift powder pattern, with the broad Gaussian component centered about the spectrometer frequency corresponding to the broad underlying resonance. The fit with the powder pattern gave a mean-square error of approximately one-half that of the two-Gaussian fit. The components of the chemical shift tensor derived from the best fit are  $\omega_1 = 419$  ppm,  $\omega_2 = 447$  ppm, and  $\omega_3 = 522$  ppm, and the broadening is 19 ppm. The data and fit are shown in Figure 5. The quality of this fit, the arguments above, and the line narrowing observed under magic-angle spinning lead us to conclude that chemical or Knight shift anisotropy dominates the line shape of the narrow resonance.

The line position, or first moment, has contributions from several sources. Comparison of the first moment of spectra taken at two different field strengths (535 versus 475 ppm for sample II) shows that the shifts expressed in ppm are not constant. If second-order quadrupolar effects were to dominate the isotropic resonance position, we would expect a higher frequency shift at lower field strength, as observed. However, we observe only a 12% change in position for a 40% change in inverse field strength. Therefore, we suggest that second-order quadrupolar effects are noticeable but not dominant and that the shift is primarily a chemical or Knight shift.

What is the origin of the changes in first and second moment with temperature (Figure 3)? Again, if they were due exclusively to second-order quadrupole effects, the large shift of the first moment to lower frequency as the temperature was decreased below  $T_c$  would imply a smaller quadrupolar coupling constant and correspondingly a higher degree of symmetry in the crystal structure below  $T_c$ . X-ray diffraction has shown that no significant change in the lattice parameters occurs at or below the critical temperature.<sup>29</sup> Also, nuclear quadrupole resonance spectra of the lanthanum nuclei show no change in satellite splitting on going through the superconducting transition region, indicating no change in the electric field gradient at the lanthanum nuclei.<sup>28</sup> Hence we conclude that second-order quadrupolar effects are not responsible for the observed changes in the first and second moments with temperature.

On the basis of the above discussion and the fact that the chemical shift is usually not a function of temperature,<sup>25</sup> we speculate that the Knight shift is responsible

(29) Cava, R. J.; Santoro, A.; Johnson, D. W. Jr.; Rhodes, W. W. *Phys. Rev. B* 1987, 35, 6716.

(30) Coretsopoulos, C.; Lee, H. C.; Ramli, E.; Reven, L.; Rauchfuss, T. B.; Oldfield, E. *Phys. Rev. B* 1989, 39, 781.

(31) The charge values used were: +3 for La, +2 for Sr, +2.15 for Cu, and -2 for O.

(32) Van Vleck, J. H. *Phys. Rev.* 1948, 74, 1168.

(33) Cohen, M. H.; Rief, F. *Solid State Phys.* 1957, 5, 321.

for the temperature-dependent behavior of the first moment at the axial oxygen site. It is difficult to estimate the diamagnetic contribution to the shift (arising from  $\chi_{\text{orb}}$  and from chemical shift effects), although if one postulates Yosida behavior,<sup>13</sup> then the exponential dependence of frequency on temperature below  $T_c$  could be extrapolated to 0 K and the intercept would be the diamagnetic contribution. Our data are too limited and contain too much scatter for this analysis. The shift shown in Figure 3 is positive and not a strong function of temperature above the transition temperature, though it increases gradually as the temperature decreases. It increases more sharply with an upturn in the range 40–80 K, just above  $T_c$ , and then rapidly moves to lower frequency as the temperature is decreased below  $T_c$ . It is interesting to note that the upturn in the frequency shift just above  $T_c$  is significantly more pronounced in sample I, which is a better superconductor according to the susceptibility data shown in Figure 1. At present we do not understand the significance of this upturn, although we feel it must be associated with the onset of superconductivity.

The observed decreasing Knight shift in the superconducting state could correspond to an increasing relative contribution from the non-s electronic part of the susceptibility, weighted with a negative coefficient  $\gamma$ . Because paired carriers do not contribute to the susceptibility, the observed decrease in Knight shift below  $T_c$  would imply, under the simplest interpretation, that  $\sigma$ -hybridized carriers are involved in pair formation in the superconducting state. This is consistent with the conclusions mentioned above for both oxygen sites in  $\text{YBa}_2\text{Cu}_3\text{O}_{7-x}$ .<sup>22,23</sup> In summary, our observations show that the spin susceptibility of the axial oxygen site in  $\text{La}_{1.85}\text{Sr}_{0.15}\text{CuO}_4$  is influenced at temperatures just above and below the onset of superconductivity. Further interpretation of the temperature dependence of the Knight shift at this axial oxygen site, including the significance of the upturn in the shift just above the critical temperature, as well as an investigation of the Knight shift at the planar oxygens, may provide additional insights into the identification of the charge carriers in the superconducting state.

The second moment of the axial oxygen resonance, shown in Figure 3, bottom, increases with decreasing temperature down to and below  $T_c$ . Careful analysis of the data shows exponential or high-order power law behavior, with no discontinuity but a slight change in parameters upon passing through the superconducting transition region. At present we do not understand the origin of this broadening, and although one is tempted to consider broadening mechanisms frequently associated with type II superconductors,<sup>34</sup> the change in our linewidth data at  $T_c$  is not convincing enough to pursue this analysis.

We now turn to a discussion of the relaxation behavior. Inspection of Figure 4 clearly shows two different regimes of temperature dependence of the spin-lattice relaxation, neither of which yields the anticipated Korringa behavior. Below  $T_c$  the relaxation time ( $T_1$ ) is temperature inde-

pendent and equal to approximately 940 ms. Others have found that the lanthanum-139 relaxation times in  $\text{La}_{1.85}\text{Sr}_{0.15}\text{CuO}_4$  are roughly constant below  $T_c$  at 530 ms.<sup>35</sup> Because the 475 ppm resonance overlaps the broad satellite transition of the lanthanum nuclei and the lanthanum nuclei have shorter relaxation times, it is likely that the lanthanum nuclei serve as a "bath" for oxygen relaxation, thus obfuscating the details of the superconducting phenomenon. In fact, in the experiments performed with shorter delays, proportionally more of the line shape was contributed to by the broad underlying resonance, confirming that the relaxation times of the lanthanum-139 nuclei or of the nuclei associated with the broad oxygen-17 resonance at 1800 ppm are significantly shorter than those of the axial oxygen-17 nuclei at 475 ppm. Above the critical temperature our oxygen-17 spin-lattice relaxation data may be fit to the following expressions:

$$1/T_1 = 4.0 \exp((-81 \text{ cal/mol})/RT) \quad R^2 = 0.983 \quad (4a)$$

$$1/T_1 = 0.8 + (1.7 \times 10^{-2})T - (2.5 \times 10^{-5})T^2 \quad R^2 = 0.960 \quad (4b)$$

Comparison of our results to the lanthanum data is still relevant above  $T_c$  because the lanthanum resonance still overlaps the oxygen resonance. The lanthanum nuclear spin-lattice relaxation times decay above  $T_c$  to less than 50 ms at 298 K, with  $1/T_1 T$  a linear function of temperature.<sup>35</sup> This behavior was attributed to quadrupolar relaxation mechanisms. Our oxygen relaxation times are longer yet do decrease with increasing temperature. Our data, however, do not fit well to a linear plot of  $1/T_1 T$  versus  $T$  ( $R^2 = 0.89$ ). The observed exponential and power law fits are more consistent with relaxation via direct or indirect coupling of the quadrupolar oxygen-17 nuclei to phonon modes.<sup>25</sup>

In summary, we have observed a shift to lower frequency in the oxygen-17 resonance of the axial oxygen sites in  $\text{La}_{1.85}\text{Sr}_{0.15}\text{CuO}_4$  as temperatures are lowered below the superconducting transition temperature. We conclude that the observed shift contains Knight shift contributions and that the spin susceptibility of this axial oxygen site is affected by the onset of superconductivity. The temperature dependence of the relaxation rates do not yield new information about the electronic structural changes associated with superconductivity; rather, they are dominated by phenomena typical of quadrupolar nuclei in solids.

**Acknowledgment.** This work was supported by the Director, Office of Basic Energy Sciences, Materials Science Division, of the U.S. Department of Energy under Contract DE-AC03-76SF00098. We acknowledge H. zur Loya, W. Ham, and Prof. A. Stacy in the Department of Chemistry for the preparations of the sample precursors and for the magnetic measurements, C. Chang at Mobil Research for the X-ray data, and S. Adler in the Department of Chemical Engineering for the NMR spectrum at 36 MHz.

**Registry No.**  $\text{La}_{1.85}\text{Sr}_{0.15}\text{CuO}_4$ , 107472-96-8;  $^{17}\text{O}$ , 13968-48-4.

(34) MacLaughlin, D. E. *Solid State Phys.* 1976, 31, 1.

(35) Butaud, P.; Ségransan, C.; Berthier, C.; Berthier, Y.; Paulsen, C.; Tholence, J. L.; Lejay, P. *Phys. Rev. B* 1987, 36, 5702.